Available online at www.sciencedirect.com
SCIENCE DIRECT
International Journal of Mass Spectrometry 245 (2005) 94–107
International Journal of Mass Spectrometry
www.elsevier.com/locate/ijms

Molybdenum isotope ratio measurements on geological samples by MC-ICPMS

Dmitry Malinovsky [a,*], Ilia Rodushkin [b], Douglas C. Baxter [b], Johan Ingri [a], Björn Öhlander [a]

[a] *Division of Applied Geology, Luleå University of Technology, S-971 87 Luleå, Sweden*
[b] *Analytica AB, Aurorum 10, S-977 75 Luleå, Sweden*

Received 2 June 2005; received in revised form 21 July 2005; accepted 21 July 2005
Available online 26 August 2005

Abstract

A method using multiple-collector inductively coupled plasma mass spectrometry (MC-ICPMS) for the precise measurement of Mo isotopic composition in geological samples has been developed. Purification of Mo for isotope ratio measurements was realized by ion-exchange chromatography using the chelating resin Chelex-100. This technique allows an efficient separation of Mo from an excess of Fe in samples and at the same time provides quantitative recovery of Mo. Instrumental mass discrimination is corrected by using Pd spiking and normalization to the $^{105}Pd/^{104}Pd$ ratio. Mo isotope ratios of samples are expressed in per mil relative to those of the bracketing in-house Mo standard. The long-term reproducibility at the two standard deviation level is 0.04, 0.06, 0.08 and 0.14‰ for $^{96}Mo/^{95}Mo$, $^{97}Mo/^{95}Mo$, $^{98}Mo/^{95}Mo$ and $^{100}Mo/^{95}Mo$ ratio measurements, respectively. The technique has been applied to measurement of the Mo isotopic composition of freshwater sediments and molybdenites. Mass-dependent variations in the isotopic composition of Mo spanning the range of ∼2.2‰ in terms of the $^{97}Mo/^{95}Mo$ ratio for two sediment columns from different redox environments have been resolved. These results show that Mo isotope effects induced by geochemical processes operating during weathering and transport of Mo to the oceans should be quantified in order to interpret global Mo isotope budget and make use of stable Mo isotopes as proxy for redox conditions in the geological past.

Keywords: Mo stable isotopes; Fractionation; Sediments; MC-ICPMS

1. Introduction

Molybdenum is an element of considerable geochemical and cosmochemical importance. It is a relatively rare element and in its compounds exhibits all oxidation states from 2− to 6+. Mo has seven naturally occurring isotopes, namely ^{92}Mo, ^{94}Mo, ^{95}Mo, ^{96}Mo, ^{97}Mo, ^{98}Mo and ^{100}Mo with relative abundances ranging from 9.2 to 24.2% [1]. Applications of Mo concentration and isotope data have been recently reviewed by Anbar [2]. In the context of aqueous geochemistry, a field of rapidly developing Mo research, Mo in marine and freshwater sediments is a powerful proxy for oxygen content and redox state of waters at the time of sediment formation [2–7]. This application makes use of the unusual chemistry of Mo. Thermodynamic data suggest that Mo should have an oxidation state of 6+, Mo(VI), in oxygenated waters. In this oxidation state, the metal is strongly hydrolyzed, and its speciation is dominated by the molybdate anion, MoO_4^{2-}. The molybdate anion has conservative-type behaviour and interacts weakly with suspended particulate matter. As a consequence, Mo is the most abundant transition metal in seawater and has an oceanic residence time of $\sim 8 \times 10^5$ years, which is much longer than the mixing time of the oceans [8]. However, under reducing conditions the stable oxidation state is Mo(IV), and molybdenum sulfide minerals are favoured thermodynamically in the presence of H_2S. Molybdenum is so rapidly removed from solution under anoxic conditions in the presence of H_2S that ocean sediments accumulating today beneath anoxic and sulfidic

* Corresponding author. Tel.: +46 920491384; fax: +46 920491199.
E-mail address: dima@ltu.se (D. Malinovsky).

1387-3806/$ – see front matter © 2005 Elsevier B.V. All rights reserved.
doi:10.1016/j.ijms.2005.07.007

waters account for up to 50% of the annual removal flux of Mo from the oceans even though such waters cover a small percentage of the modern seafloor (<0.5%) [2,4]. Given that Mo has low lithogenic background in sediments, these authigenic enrichments in reducing settings have been used as an indicator of anoxia of deep waters.

Recent improvements in mass spectrometry have facilitated precise measurements of Mo isotope ratios [9–12]. This has increased the attractiveness of Mo isotopes as a geochemical tool. The published data on variations in isotopic composition of Mo have demonstrated that stable isotopes of Mo can be used efficiently to complement its concentration data in paleoredox reconstructions [13–16]. It has been shown that marine sedimentary material formed in different redox environments have distinct Mo isotope signatures. Sediments formed under oxic conditions, including pelagic clays and Fe–Mn crusts, are isotopically lighter than parent seawater by ∼2.0‰ in terms of $^{97}Mo/^{95}Mo$ ratio [2]. On the other hand, sediments overlain by anoxic H_2S bearing waters have the isotopic composition of Mo close to that of seawater or slightly lighter. Variations in Mo isotopic composition for a limited number of analyzed molybdenites are within 1‰ in terms of $^{97}Mo/^{95}Mo$ ratio, whereas those for a number of basalts and granites are less than 0.5‰ [2,10,14,15,17]. This led to the preliminary suggestion that variations in isotopic composition of Mo input from the continents to the oceans are small compared to those documented for marine settings [2,15].

Precise Mo isotope ratio measurements have been performed using positive ion thermal ionization mass spectrometry (TIMS) [10,17] and MC-ICPMS [9,11–16]. The latter technique is experiencing a rapid growth and provides precision of isotope ratio measurements comparable or even superior to TIMS. MC-ICPMS is more suitable than TIMS for the acquisition of precise isotope ratio data for elements with high first ionization potentials, such as Mo (7.1 eV), and offers such clear advantage as high sample throughput. However, instrumental mass bias effects in MC-ICPMS are larger than those encountered in TIMS, but are considered to be more temporally stable during measurement and can be corrected for adequately. Double spiking [12,14,15] and doping with an external element (Zr or Ru) [11,13,16] have been used previously in order to correct for mass bias affecting Mo isotopes during MC-ICPMS measurements. Zr has isobaric interferences of $^{92}Zr^+$ on $^{92}Mo^+$, $^{94}Zr^+$ on $^{94}Mo^+$ and $^{96}Zr^+$ on $^{96}Mo^+$, whereas Ru has isobaric interferences of $^{98}Ru^+$ on $^{98}Mo^+$ and $^{100}Ru^+$ on $^{100}Mo^+$. Doping of sample solutions with either Zr or Ru will thus limit the number of interference-free Mo isotope ratios to be measured. The double spike method, using highly enriched ^{100}Mo and ^{97}Mo or ^{94}Mo isotopes, is advantageous in that its application allows relaxing the requirement for quantitative recovery of Mo from the sample matrix, while resolving effectively instrumental mass bias. However, the limitations of double spiking are complexities associated with accurate addition of the spike and data reduction.

Purification of Mo from sample matrix is critical requirement for precise Mo isotope ratio measurements in order to reduce potentially interfering ions [18,19]. The purification of Mo implies that concomitant matrix elements should be reduced down to trace levels [19]. We observed that, for geological samples with high Fe and low Mo contents, such as freshwater sediments, the separation of Mo from Fe while providing quantitative yield of Mo is a significant analytical challenge. The purification methods used in previous studies were not efficient enough in meeting the aforementioned requirements. These methods include a two-column ion-exchange chromatography using anion-exchange column for separation of Zr and Mn from Mo followed by cation-exchange column for separation of Fe from Mo [13] and solvent extraction followed by ion-exchange chromatography [20].

In this study, we have developed a chemical purification technique and MC-ICPMS measurement protocol that permit the precise determination of Mo isotope compositions for geological samples. The purification of Mo was realized by ion-exchange chromatography using the chelating resin Chelex 100. This method has been found effective in the separation of Mo from most matrix elements, including Fe. The MC-ICPMS measurement protocol utilizes the external normalization technique using Pd to correct for instrumental mass bias. This permits measurements of six Mo isotopes, while sacrificing ^{92}Mo due to mechanical limitations of collectors positioning in the case of wide mass coverage on the instrument used. The developed method has been applied successfully to measurements of Mo isotopic variations in freshwater sediment columns and in molybdenites.

2. Experimental

2.1. Instrumentation

Prior to Mo isotope ratio measurements, the concentrations of Mo, Zr, Fe, Ru and a suite of other matrix elements in the samples were determined by single collector inductively coupled plasma sector field mass spectrometry (ICP-SFMS; the Element, Thermo Finnigan, Bremen, Germany). Typical operating conditions for this instrument are reported elsewhere [21]. Mo isotope ratio measurements were performed using the Neptune MC-ICPMS (Thermo Finnigan). The instrument incorporates a double focusing, sector field mass spectrometer. The Neptune has three switchable entrance slits located before the electrostatic analyzer with slit widths of 250, 30 and 16 μm resulting in low, “medium” and “high” resolution modes. For mass resolution definition in this MC-ICPMS instrument, Δm is defined as the mass difference between the points where the intensity on the leading edge of the peak changes from 5 to 95% of the maximum [22]. The resolving power is then defined as follows:

Table 1
Typical operating conditions for the Neptune MC-ICPMS during this study

RF power (W)	1300
Acceleration potential (V)	~10000
Ion lens settings	Optimized for maxim intensity of Mo signal
Sampler and skimmer cones	Ni, 1.1 and 0.8 mm orifice diameter, respectively
Argon gas flow rate (l/min)	
Coolant	16
Auxiliary	0.8
Nebulizer	~1.1 (Optimized before each measurement session)
Sample uptake rate (ml/min)	~0.25
Mass resolution	~400

$$R_{\text{power(5,95\%)}} = \frac{m}{\Delta m} = \frac{m}{m(5\%) - m(95\%)} \quad (1)$$

Low resolution mode was used in this study with $R_{\text{power(5,95\%)}}$ ~400. The Neptune is equipped with eight adjustable Faraday cups and one fixed centre cup. To increase the sensitivity, the instrument is also equipped with a guard electrode that improves the ion transmission efficiency and prevents secondary discharges in ICP. After plasma ignition, ~1 h period of stabilization was allowed before making any measurements. Prior to each measurement session, the instrument was carefully tuned to maximize the intensity of the Mo signal by adjusting the torch position, gas flows and lens voltages. Typical operating conditions adopted for the instrument are summarized in Table 1. Samples and standards were prepared in 0.3 M HNO_3 solution and introduced into the plasma through the stable introduction system consisting of tandem quartz spray chamber arrangements (cyclone + Scott double pass), a micro-concentric PFA nebulizer, and a peristaltic pump (Perimax 12, SPETEC, Erding, Germany) operating at a flow rate of about 0.25 ml min^{-1}.

$^{94}Mo^+$, $^{95}Mo^+$, $^{96}Mo^+$, $^{97}Mo^+$, $^{98}Mo^+$, $^{100}Mo^+$, $^{104}Pd^+$ and $^{105}Pd^+$ ion beams were collected by Faraday cups at Low 4, Low 3, Low 2, Low 1, Central, High 1, High 3 and High 4 positions, respectively. All analyses were made in a sequence of isotope standard, "unknown" sample, isotope standard and so on. Concentrations of samples and bracketing standards were matched to within 20%. The analyses were conducted in the static mode. Each sample measurement consisted of eight blocks, each block comprising five cycles of ~5.5 s duration. All samples and standards were analyzed in duplicate, giving a total analysis time per sample of ~10 min. The sensitivity for $^{98}Mo^+$ was ~7 V per mg l^{-1} Mo. After semi-quantitative analysis by ICP-SFMS, the Mo samples were diluted to 1 or 2 mg l^{-1} Mo with 0.3 M HNO_3 and spiked with Pd at 0.5 or 1 mg l^{-1} Pd, respectively, followed by isotope ratio measurements by MC-ICPMS.

2.2. Data processing

The on-line data processing included calculation of the ion beam intensity ratios and filtering of outliers by a 2σ test. Further statistical treatment of the data was performed off-line. For the presentation of results, δ-notation is utilized [2], as defined by the relationship:

$$\delta^x\text{Mo} \left[\frac{(^x\text{Mo}/^{95}\text{Mo})_{\text{sample}}}{(^x\text{Mo}/^{95}\text{Mo})_{\text{standard}}} - 1 \right] \times 1000 \text{ ‰} \quad (2)$$

where x is ^{94}Mo, ^{96}Mo, ^{97}Mo, ^{98}Mo or ^{100}Mo isotope, respectively, in the measured ratios for sample and standard (High Purity Mo standard), corrected for instrumental mass discrimination using Pd.

2.3. Samples and reagents

The sediments analyzed in this work were collected in two freshwater lakes, Kutsasjärvi and Vettasjärvi, in northern Sweden. Sampling of these sediments was performed in the deepest part of each lake by using a gravity corer that permits collection of a sediment column. Immediately after sampling, the sediment cores were sliced into 1 cm thick layers, which were placed in acid-washed Petri dishes and kept frozen until analysis.

Two molybdenite powders, HLP-5 and JDC, that have been used as reference materials in a number of studies on Re–Os dating of molybdenites and other geological samples [23,24], have been acquired from the Chinese National Research Center of Geoanalysis. One of the molybdenites powders, HLP-5, was from a carbonate vein-type molybdenum–lead deposit in the Jinduicheng-Huanglongpu area of Shaanxi Province, China. The second material, JDC, was from the Tuwu-Yandong porphyry copper deposit, China. A third sample of molybdenite, Kåtaberget, was obtained from molybdenite mineralized aplites associated with Proterozoic granites in northern Sweden.

Analytical grade nitric acid (65%, Merck, Darmstadt, Germany) was used throughout the study after additional purification by sub-boiling distillation in a quartz still. Hydrochloric (30% Fluka, Steinheim, Germany, analytical-plus grade) and hydrofluoric (48%, analytical plus grade, Sigma–Aldrich, Germany) acids were used without additional purification. Chelating ion-exchange resin Chelex® 100 (Na-form), 200–400 mesh, 0.4 meq ml^{-1}, 0.6 ml g^{-1} (Bio-Rad, analytical grade) was used for purification of Mo. Calibration and internal standard solutions were prepared by diluting single element standard solutions (SPEX Plasma Standards, Edison, NJ, USA). The dilution of samples and standards was performed using distilled Milli-Q water (Millipore Milli-Q, Bedford, USA). A Mo standard solution (High-Purity Standards, lot #320304, Charleston, SC 29423, USA) was employed as the in-house standard for measurement of Mo isotope ratios.

2.4. Sample decomposition

Molybdenum can be extracted from natural samples by applying either total decomposition or selective extraction

procedures. A total decomposition procedure was used for samples of molybdenite because this mineral contains no other major constituents, apart from sulfur. Approximately 0.1 g of the sample has been dissolved by using aqua regia in Teflon beakers on a hot plate followed by gentle evaporation to dryness and reconstitution in 0.3 M HNO_3.

By applying different extraction procedures it is possible to liberate selective fractions of Mo from its total content in a sample. In this study we used a reductive hydroxylamine-hydrochloride leach in order to dissolve Mn and Fe oxide minerals while not attacking the detrital silicate phase [25,26]. Mn and Fe oxides are important hosting phases for Mo in freshwater sediments. Replicated pseudo-total microwave-assisted digestion of sub-samples of these sediments by using a mixture of aqua regia and HF demonstrated that Mo associated with the non-detrital phase (organics and Fe–Mn oxides) constitutes more than 95% of pseudo-total content. Prior to leaching, the sediment samples were ashed in order to decompose organic C. Organic material was found to affect negatively the performance of subsequent ion-exchange purification of Mo. The complete sequence of the extraction procedure is as follows. Approximately 0.5 g of powdered sample was ashed at 550 °C during ∼16 h. After cooling down, the sample was carefully transferred to a Teflon beaker and extracted with 20 ml of ∼4 M HCl acid with addition of ∼20 mg of hydroxylamine hydrochloride. The beaker was kept on a hot plate at 50 °C for 3 h. The sample solution was then transferred into polypropylene tubes, centrifuged, and the aqueous phase was decanted. Molybdenum released to solution is therefore represented by fractions associated with both Fe–Mn oxides and organic matter. The solutions were dried down in Teflon beakers and re-dissolved in 0.3 M HNO_3. These samples are ready for purification of Mo prior to mass spectrometric measurements.

2.5. Ion exchange procedure for purification of Mo

Purification of Mo is necessary in order to eliminate potential spectral interferences and minimize matrix effects during MC-ICPMS measurements. Molybdenum from most geological samples has to be purified because Mo is typically a minor or trace constituent of the sample matrix. The only major exception is molybdenite, MoS_2, a mineral in which Mo is the major constituent; other elements, including Zr and Fe, are present at negligible levels relative to Mo. Therefore, no purification has been applied after decomposition of molybdenites in this study.

Effective separation of Mo from Fe and a suite of other concomitant elements was realized by using chelating ion-exchange chromatography according to a procedure modified from Riley and Taylor [27]. Ion-exchange columns were prepared from 10 ml disposable pipette tips, loaded with ∼3 ml of the ion-exchange resin Chelex® 100 held in place with small plugs of cotton wool. Prior to loading into columns, the resin was aliquoted into 12 ml polypropylene tubes and allowed to equilibrate with 5 ml of 6 M NH_3 over night for the purpose of cleaning, because the final elution of Mo from the ion-exchange resin was realized using 6 M NH_3. The resin was separated by centrifugation, splashed with Milli-Q water and transferred into the column. Further details of cleaning, conditioning, sample loading and elution of Mo for this chromatographic procedure are shown in Table 2. Molybdenum was eluted from the column in 12 ml of 6 M NH_3 solution. The samples were then dried down on a hot plate and re-dissolved in 0.3 M HNO_3. These solutions are ready for Mo isotopic analysis and require only appropriate dilution. The efficiency of purification and yield of Mo have been estimated on aliquots of each sample taken before and after ion-exchange separation, and measured by ICP-SFMS. The sample preparation and ion exchange separation of Mo was carried out in a clean environment (class 1000). Procedural blanks were prepared for all sample manipulations and found to contain negligible quantities of Mo (<10 ng) relative to those of Mo in samples.

Table 2
Elution sequence for ion-exchange chromatography using Chelex-100 chelating resin, 200–400 mesh, Bio-Rad, 3 ml

Eluent	Volume (ml)	Purpose
8 M HNO_3	15	Resin cleaning
Milli-Q water	5	Resin cleaning
0.3 M HNO_3	10	Resin conditioning
0.3 M HNO_3	12	Sample load
0.07 M HCl	10	Matrix elution
0.1 M HF	50	Matrix elution
6 M NH_3	12	Mo elution

It was found possible to use the columns repeatedly. A large volume of 8 M HNO_3 (20–40 ml) was passed through the column for cleaning of the resin between sample loadings.

3. Results and discussion

3.1. Performance of chelating ion-exchange chromatography for purification of Mo

The primary challenge in purification of Mo is its separation from Fe; the latter is a major matrix constituent in freshwater sediments. Most of the samples in this study were purified in a single pass through an ion exchange column of Chelex-100 chelating resin. Due to their importance in analytical chemistry, iminodiacetic acid (IDA) chelating resins have been widely studied [28–32]. At lower pH the resin acts as an anion exchanger [31], but its structure changes with increasing pH. At pH from 2.21 to 3.99, the protonated cationic form of IDA group is dominant and the ligand can be expressed as ($–LH_3^+$). At pH over 7.41 and up to 12.30, the monovalent anionic form prevails ($–LH^-$), and at pH over 12.30 the stable form is the divalent anionic form ($–LH^{2-}$) [32].

The sample solutions loaded onto the columns in 0.3 M HNO_3 have pH ∼0.5. Under these conditions, Mo is presum-

ably present in solution as heptamolybdate ions ($Mo_7O_{24}^{6-}$) [33] that will be efficiently retained on Chelex-100 in its anion exchanger form. Elutions with 0.07 M HCl and 0.1 M HF essentially removes concomitant matrix elements co-adsorbed with Mo. Elution with 0.1 M HF is particularly efficient in removing Fe and Zr. Molybdenum is eluted with 6 M NH_3. Under these strongly alkaline conditions the speciation of Mo is MoO_4^{2-} anion [34] and it is eluted quantitatively from the resin while residual Fe remains immobile on the column.

A feature of the Chelex resin is that its volume changes when its ionic form is altered. The water uptake, or swelling, is pronounced because of low cross-linking of the resin. Substantial swelling of the resin occurs during the elution of Mo with 6 M NH_3. During initial stages of this work we observed that if ashing of organic matter was not applied, the organic C of sample solutions interacted with the resin and elution of Mo with 6 M NH_3 resulted in "clogging" of flow through the column. Elimination of organic matter by ashing has been found to be an efficacious solution to this problem.

For some samples, however, a second pass through the column was necessary in order to get rid of traces of Zr and to reduce the concentration of Fe to an acceptable level. In such cases, the ammoniacal Mo fraction eluted after the first run was dried down on a hot plate, re-dissolved in 0.3 M HNO_3 and loaded again on the same column that was pre-conditioned by 0.03 M HNO_3 prior to the load. The elution sequence described in Table 2 was repeated. The criterion for acceptable purification of Mo from Fe was Fe/Mo ratio in sample solutions <1. After purification, matrix components in sample solutions consisted of traces of Fe, Na, K, Ca and Al, but may contain elevated concentrations of Si relative to Mo. Silicon was released into solution during Mo elution by ammonia solution. The allowable levels of Si in solutions for precise Mo isotope ratio measurements will be discussed in Section 3.3.

Confirmation that the yield of Mo from the separation process is quantitative is very important in light of the finding that Mo isotopes can be fractionated during elution in ion-exchange chromatography [11]. The quantitative recovery of Mo was therefore ensured during the ion-exchange separation in this study. Absence of artificially introduced isotopic fractionation of Mo due to its incomplete recovery after the ion-exchange chromatography was confirmed by replicated processing of Mo standard and some sediment samples through the ion-exchange purification procedure and measurements of Mo isotopic composition by MC-ICPMS.

3.2. Spectral interferences

The determination of Mo isotope ratios can be dramatically affected by spectral interferences. Potential interfering ions could be present in the sample or formed during the process of the measurement itself. Interferences can appear from isobaric overlapping, polyatomic ion formation, doubly charged ions and refractory oxide formation. The major potential interferences on Mo isotopes as well as on $^{104}Pd^+$ and $^{105}Pd^+$ are given in Table 3.

As seen in Table 3, critical elements prone to formation of severe interferences on Mo isotopes and on the normalizing $^{105}Pd/^{104}Pd$ ratio include Zr, Ru, Fe, Mn, Zn, Cu, Ni, Co and Cr. Except for Ru, which has extremely low concentrations in most matrices, these elements are abundant in natural geological samples. Moreover, most of the interferences originating from these elements could not be resolved instrumentally even if high resolution mode is utilized. This highlights the importance of the off-line chemical purification scheme for samples in order to minimize the possibility of interference formation from Zr, Fe, Mn, Cu, Ni, Zn, Co and Cr. We believe that Mo purification procedure described above is adequate for reducing the aforementioned elements to insignificant concentration levels.

To quantify the influence of residual Fe in sample solutions following purification, interference experiments have been carried out using synthetic solutions of our in-house Mo standard and Fe mixed with varying Fe/Mo ratios. As $^{105}Pd/^{104}Pd$ ratio was utilised in this work for mass bias correction, it is important to ensure interference-free measurement of this isotope ratio as well. The same interference experiments have been performed using Mo solutions doped with equal Pd and varying Cu concentrations in order to evaluate the influence of the $^{65}Cu^{40}Ar^+$ interference occurring with ^{105}Pd on the measured Mo isotope ratios after normalization to the $^{105}Pd/^{104}Pd$ ratio.

As plotted in Fig. 1a, the results show that the effect of Fe concentration in the sample solution on the measured Mo isotope ratios is negligible for Fe/Mo ratios less than unity. However, the measured Mo isotope ratio shows a clear dependency on Fe when Fe/Mo >5. An interesting observation is that the use of Pd as a normalizing element for mass bias correction allows substantial reduction in the drift of measured Mo isotope ratios where samples were doped heavily with Fe. The results shown in Fig. 1a imply that, under working conditions used in this study, reduction of Fe concentration in sample solutions down to Fe/Mo $\leq$1 is adequate for precise and accurate Mo isotope ratio measurements.

Fig. 1b shows an illustration of possible artifacts in Mo isotope ratio measurements when employing Pd as an external element for mass bias correction. The effect of Cu concentration in the sample solution on the measured Mo isotope ratios is negligible for Cu/Pd ratios below unity. Deviations of δ-values for Mo isotope ratios become pronounced when Cu/Pd ratios exceed two; further increases result in dramatic artifacts.

The probability of spectral interferences originating from doubly charged ions (Os, Pt, Pb and Hg) and from refractory oxides (Se, Ge, Sr and Y) is considered very low because most of these elements are present at trace level in geological samples and are readily separated from Mo during the purification procedure. Concentrations of these elements in the sample solutions analyzed by MC-ICPMS in

Table 3
List of major potential interferences on Mo isotopes, ^{104}Pd and ^{105}Pd

Mass	Oxide ions	Argide ions	Nitrogen monoxide ions	Chloride ions	Isobars	Doubly charged ions
^{92}Mo	^{76}Se^{16}O$^+$ (0.093); ^{76}Ge^{16}O$^+$ (0.074); ^{75}As^{17}O$^+$ (0.0004)	^{38}Ar^{54}Fe$^+$ (0.00004); ^{38}Ar^{54}Cr$^+$ (0.00001)	^{62}Ni^{14}N^{16}O$^+$ (0.036); ^{59}Co^{15}N^{18}O$^+$ (0.00001)	^{57}Fe^{35}Cl$^+$ (0.017); ^{55}Mn^{37}Cl$^+$ (0.24)	^{92}Zr$^+$ (0.17)	^{184}W^{++}(0.14) ^{184}Os^{++}(0.0002)
^{94}Mo	^{78}Se^{16}O$^+$ (0.24)	^{56}Fe^{38}Ar$^+$ (0.0006); ^{54}Fe^{40}Ar$^+$ (0.058); ^{58}Ni^{36}Ar$^+$ (0.002); ^{54}Cr^{40}Ar$^+$ (0.023)	^{64}Zn^{14}N^{16}O$^+$ (0.48); ^{63}Cu^{15}N^{16}O$^+$ (0.003); ^{62}Ni^{14}N^{18}O$^+$ (0.00007)	^{59}Co^{35}Cl$^+$ (0.76); ^{57}Fe^{37}Cl$^+$ (0.005)	^{94}Zr$^+$ (0.17)	^{188}Os^{++}(0.13)
^{95}Mo	^{78}Se^{16}OH$^+$ (0.24)	^{55}Mn^{40}Ar$^+$ (0.99); ^{57}Fe^{38}Ar$^+$ (0.00004); ^{59}Co^{36}Ar$^+$ (0.003)	^{65}Cu^{14}N^{16}O$^+$ (0.31); ^{64}Zn^{15}N^{16}O$^+$ (0.002)	^{58}Ni^{37}Cl$^+$ (0.16); ^{58}Fe^{37}Cl$^+$ (0.0007)		^{190}Os^{++}(0.26)
^{96}Mo	^{80}Se^{16}O$^+$ (0.49)	^{56}Fe^{40}Ar$^+$ (0.91); ^{58}Ni^{38}Ar$^+$ (0.0004)	^{65}Cu^{15}N^{16}O$^+$ (0.001); ^{66}Zn^{14}N^{16}O$^+$ (0.28); ^{64}Ni^{14}N^{18}O$^+$ (0.00002)	^{61}Ni^{35}Cl$^+$ (0.009); ^{59}Co^{37}Cl$^+$ (0.24)	^{96}Zr$^+$ (0.03); ^{96}Ru$^+$ (0.06)	^{192}Os^{++}(0.41); ^{192}Pt^{++}(0.008)
^{97}Mo	^{80}Se^{16}OH$^+$ (0.49)	^{57}Fe^{40}Ar$^+$ (0.06); ^{59}Co^{38}Ar$^+$ (0.06); ^{61}Ni^{36}Ar$^+$ (0.00004)	^{65}Cu^{14}N^{18}O$^+$ (0.0006)	^{60}Ni^{37}Cl$^+$ (0.063)		^{192}Pt^{++}(0.33)
^{98}Mo	^{82}Se^{16}O$^+$ (0.08)	^{58}Ni^{40}Ar$^+$ (0.68); ^{58}Fe^{40}Ar$^+$ (0.058)	^{68}Zn^{14}N^{16}O$^+$ (0.19)	^{63}Cu^{35}Cl$^+$ (0.52); ^{61}Ni^{37}Cl$^+$ (0.003)	^{98}Ru$^+$ (0.02)	^{196}Pt^{++}(0.25)
^{100}Mo	^{84}Sr^{16}O$^+$ (0.006)	^{60}Ni^{40}Ar$^+$ (0.261); ^{64}Zn^{36}Ar$^+$ (0.002)	^{68}Zn^{14}N^{18}O$^+$ (0.0004); ^{69}Ga^{15}N^{16}O$^+$ (0.001); ^{70}Ge^{14}N^{16}O$^+$ (0.21)	^{63}Cu^{37}Cl$^+$ (0.17);	^{100}Ru$^+$ (0.13)	^{200}Hg^{++}(0.23)
^{104}Pd	^{88}Sr^{16}O$^+$ (0.82)	^{64}Ni^{40}Ar$^+$ (0.009); ^{64}Zn^{40}Ar$^+$ (0.48)	^{74}Ge^{14}N^{16}O$^+$ (0.36)	^{67}Zn^{37}Cl$^+$ (0.01); ^{69}Ga^{35}Cl$^+$ (0.45)	^{104}Ru$^+$ (0.19)	^{208}Pb^{++} (0.52)
^{105}Pd	^{89}Y^{16}O$^+$ (0.99)	^{65}Cu^{40}Ar$^+$ (0.31) ^{67}Zn^{38}Ar$^+$ (0.00003)	^{74}Ge^{15}N^{16}O$^+$ (0.001); ^{75}As^{14}N^{16}O$^+$ (0.99)	^{68}Zn^{37}Cl$^+$ (0.045)		

The abundance of the interfering ions was calculated using data from the recent IUPAC compilation of isotope abundances [1].

the course of this work were below the limits of detection for ICP-SFMS.

3.3. Matrix effects

The term matrix effects used here refers to the phenomenon that instrumental mass discrimination during MC-ICPMS measurement varies with changes in the composition of sample solutions [18]. Matrix effects can potentially shift the Mo isotopic composition of samples along the natural mass-dependent fractionation line. Investigations here are focused on Si, since complete separation of this element was not achieved after ion-exchange chromatography, and on varying acidity levels. Interference experiments, analogous to those described in Section 3.2 above, were carried out using varying ratios of Si/Mo and concentrations of HNO_3. The results are plotted in Fig. 2. As seen from Fig. 2, the effects of Si and varying concentrations of HNO_3 acid are remarkably distinct between measurements with and without using Pd as a normalizing element for mass bias correction. For measurements using normalization to $^{105}Pd/^{104}Pd$, an excess of Si over Mo exerts no significant effect on the Mo isotope ratio measurements up to Si/Mo ratio equal to 50. In contrast, where only the sample-bracketing technique is used for mass bias correction, variation in both Si content and acidity of sample solutions can lead to significant artifacts. However, Si/Mo ratios in sample solutions purified according to the prescribed method were lower than 50. Thus, under the given working conditions, Si exerts no significant effect on the Mo isotope ratio measurements. A solution to the potential problem of high Si concentration in sample solutions is chemical purification using anion-exchange chromatography as described by Barling et al. [13].

3.4. Mass discrimination correction

Under normal operating conditions, mass discrimination in the Mo region observed in this study was approximately 2.0% per mass unit. An exponential model for its correction was evaluated and detailed descriptions of this procedure can be found elsewhere [18,19,35]. One important property of the exponential model is that any pair of isotope ratios forms a linear array in log–log space. Based on this property, correction for mass bias by using normalization to an external element assumes proportionality between the mass discrimination factors, *f*, for analyte and normalizing elements during a single measurement session. It is well recognized that the mass discrimination factors for isotopes of different elements are not identical and that they vary slightly between different measurement sessions. However, these day-to-day variations can be assumed negligible when the sample-standard bracketing is used in combination with the external normalization for the determination of the relative isotope ratios. Nevertheless, as seen in Fig. 3, despite differences in the *f*-values for $^{105}Pd/^{104}Pd$ and two most commonly used Mo isotope ratios, $^{98}Mo/^{95}Mo$ and $^{97}Mo/^{95}Mo$, over numerous measurement sessions from January to May 2005, their ratios produce well-defined linear arrays with $R^2 \sim 0.985$ ($n = 115$). Note that, since no certified materials of well-known isotopic composition are available for either Mo or Pd, the levels of instrumental mass discrimination have been computed using abundances taken from the recent IUPAC data compilation

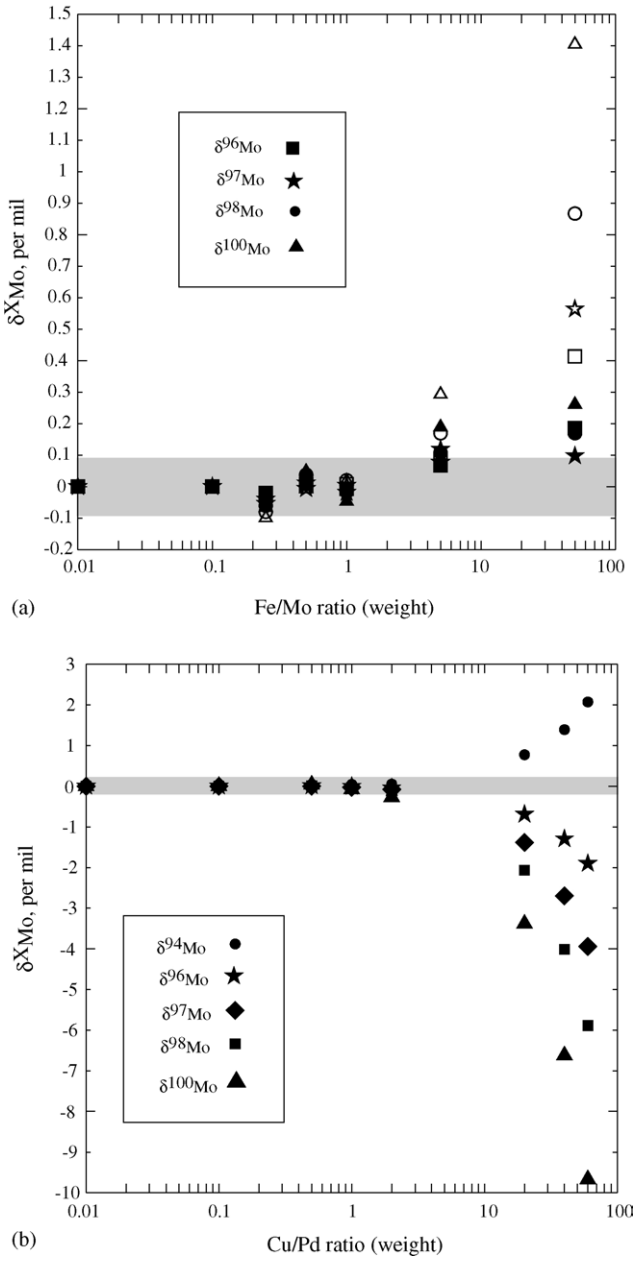

Fig. 1. Assessment of the effect of interfering signals on the measured Mo isotope ratios for the in-house Mo standard doped with: (a) Fe; (b) Cu. Filled symbols—Pd normalization using $^{105}Pd/^{104}Pd$ ratio was utilized in combination with sample-standard bracketing method for instrumental mass bias correction; open symbols—sample-standard bracketing method without Pd normalization was used. The uncertainties are the same size or smaller than the data points. The width of the grey line approximates the long-term reproducibility of the $^{98}Mo/^{95}Mo$ ratio at a level of twice the standard deviation.

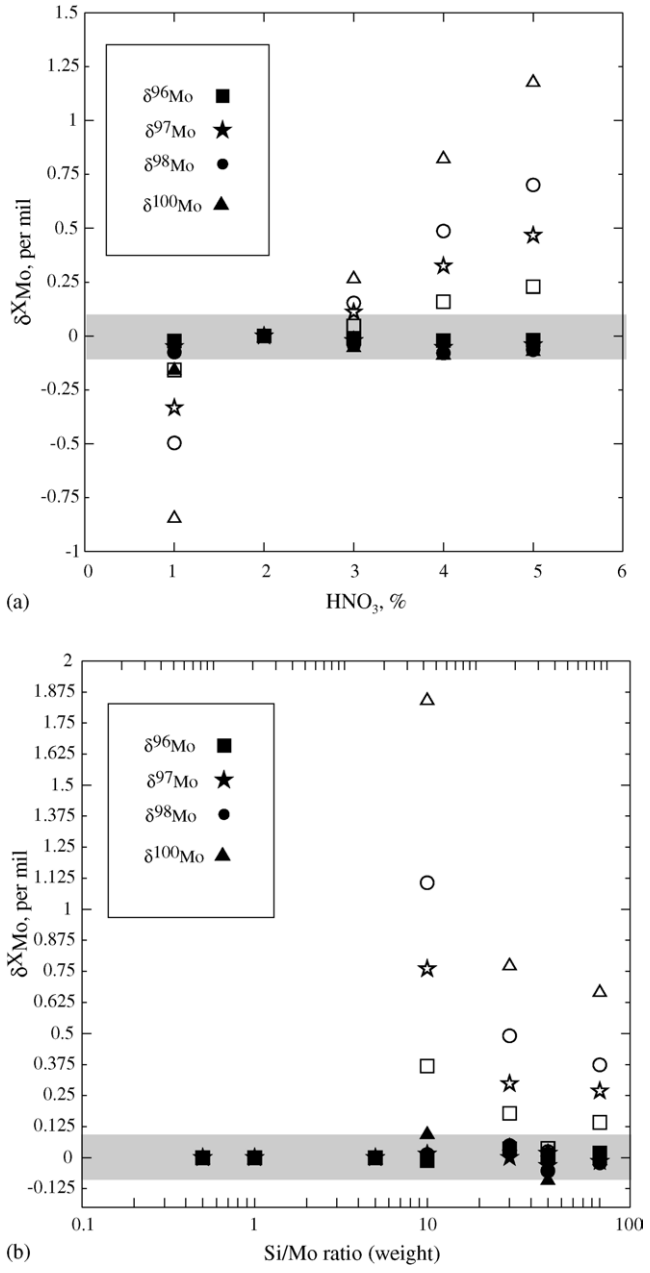

Fig. 2. Plots showing the effects of matrix chemistry on the measured Mo isotope ratios for the in-house Mo standard with: (a) varying levels of HNO_3 acid matrix; (b) varying concentrations of residual matrix element, Si. Filled symbols—Pd normalization using $^{105}Pd/^{104}Pd$ ratio was utilized in combination with sample-standard bracketing method for instrumental mass bias correction; open symbols—sample-standard bracketing method without Pd normalization was used. The uncertainties are the same size or smaller than data points. The width of grey line approximates the long-term reproducibility of $^{98}Mo/^{95}Mo$ ratio at a level of twice the standard deviation.

[1]. The latter values do not necessarily represent the true isotopic composition of the standard solutions used here. Fortunately, for the purposes of drift correction and calculation of relative Mo isotope ratios, i.e., δ-values, this is of no consequence.

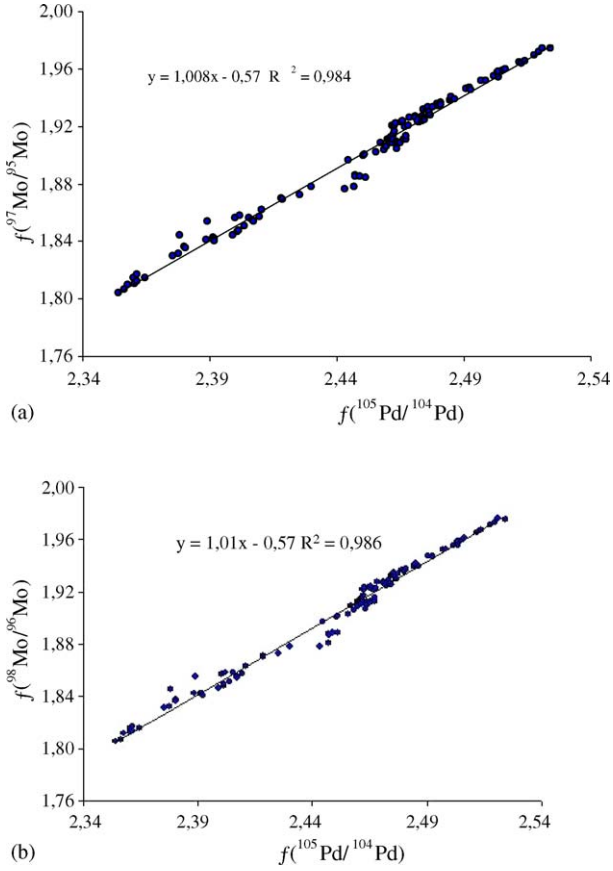

Fig. 3. Relationship between fractionation coefficients (f): (a) $f(^{97}Mo/^{95}Mo)$ vs. $f(^{105}Pd/^{104}Pd)$ and (b) $f(^{98}Mo/^{95}Mo)$ vs. $f(^{105}Pd/^{104}Pd)$ for the in-house Mo standard measurements obtained during separate analytical sessions over January–May 2005.

An approach for testing the quality of MC-ICPMS measurements can be applied following the general mass fractionation treatment of Young et al. [36]. In this approach, kinetic and equilibrium mass-dependent fractionation laws for describing the partitioning of isotopes are compared. Both laws can be formulated in the expression:

$$\delta^{97/95}\mathrm{Mo} = \left[\left(\frac{1000 + \delta^{98/95}\mathrm{Mo}}{1000}\right)^{\beta} - 1\right] \times 1000\ ‰ \tag{3}$$

where the exponent, β, takes different forms in the case of kinetic

$$\beta = \frac{\ln[m(^{95}\mathrm{Mo}/m(^{97}\mathrm{Mo})]}{\ln[m(^{95}\mathrm{Mo}/m(^{98}\mathrm{Mo})]} = 0.670 \tag{3a}$$

or equilibrium

$$\beta = \frac{\left[\frac{1}{m(^{95}\mathrm{Mo})} - \frac{1}{m(^{97}\mathrm{Mo})}\right]}{\left[\frac{1}{m(^{95}\mathrm{Mo})} - \frac{1}{m(^{98}\mathrm{Mo})}\right]} = 0.674 \tag{3b}$$

control of the process governing isotopic fractionation.

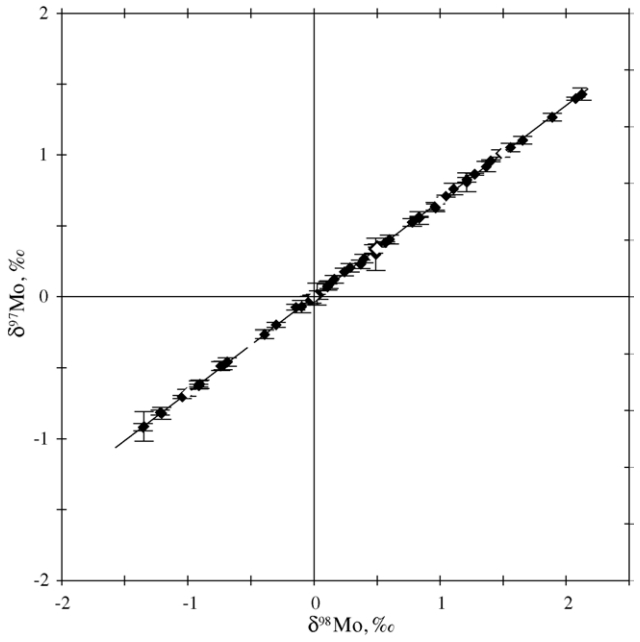

Fig. 4. Three-isotope plot of δ^{97}Mo vs. δ^{98}Mo for replicate measurements of sediment samples and molybdenites in this study ($n = 63$). Uncertainty bars are one standard deviation. The data have been corrected for instrumental mass bias using normalization to ^{105}Pd/^{104}Pd. The line through the data points was calculated using the relationship given by Eq. (3) (see Ref. [36] and text for details). The fractionation exponent derived from the measured data set ($\beta \approx b_w = 0.678 \pm 0.005$, $R^2 = 0.9997$, $n = 63$) is statistically indistinguishable from that expected for equilibrium isotope fractionation for ^{95}Mo, ^{97}Mo and ^{98}Mo, i.e., $\beta = 0.674$. The agreement of the experimentally determined fractionation exponent with the theoretical value and linearity of the array serve as an indication of insignificant spectral interferences on the measured Mo isotopes and stability of mass bias over MC-ICPMS sessions.

As this relationship defines a non-linear mass fractionation curve, linearization of the array was employed prior to linear regression analysis using weighting of both variables [36,37]:

$$\delta'^{x/95}\mathrm{Mo} = \ln\left[\frac{(^{x}\mathrm{Mo}/^{95}\mathrm{Mo})_{\mathrm{sample}}}{(^{x}\mathrm{Mo}/^{95}\mathrm{Mo})_{\mathrm{standard}}}\right] \times 1000\ ‰ \quad (4)$$

$$\delta'^{97/95}\mathrm{Mo} = a_w + b_w\delta'^{98/95}\mathrm{Mo} \quad (5)$$

The weighted intercept obtained for repeated measurements of samples of deposited sediments, molybdenites and some synthetic solutions, $a_w = (-0.3 \pm \approx 13) \times \approx 10^{-3}$ (95% confidence interval, $n = 63$) is not significantly different from zero, the latter value being defined by our in-house Mo isotope standard ($\delta'^{56}\mathrm{Fe} = \delta'^{57}\mathrm{Fe} = 0$) (Fig. 4). The weighted slope, $b_w = 0.678 \pm 0.005$ ($R^2 = 0.9997$), the experimental estimate of β, is statistically indistinguishable from that expected for equilibrium isotope fractionation. This agreement indicates the robustness of the applied mass bias correction procedure and the interference-free measurements of ^{97}Mo/^{95}Mo and ^{98}Mo/^{95}Mo ratios. The experimental fractionation exponents calculated separately for Kutsasjärvi and Vettasjärvi sediments are $\beta \approx 0.679 \pm 0.007$ ($n = 35$) and $\beta \approx 0.670 \pm 0.03$ ($n = 12$), respectively. These results would suggest that partitioning of Mo isotopes in Kutsasjärvi sediment studied is determined by equilibrium fractionation, whereas for Vettasjärvi sediment the uncertainty associated with the measurements hampers determination of the dominant control. However, it is also apparent that for reliable determination of the dominant mass fractionation laws in samples using the described approach a large set of interference-free measurements is necessary.

3.5. Precision and accuracy of isotope ratio measurements

3.5.1. Precision of isotope ratio measurements for standard solutions

The reproducibility (2σ) of Mo isotopic measurements has been assessed by repeated measurements of our in-house Mo standard collected over a period of five months in nine measurement sessions (Fig. 5). Molybdenum isotope ratios for this standard have been calculated in per mil relative to the same bracketing standards. The long-term reproducibility has been evaluated as 0.06, 0.04, 0.06, 0.08 and 0.14‰ for ^{94}Mo/^{95}Mo, ^{96}Mo/^{95}Mo, ^{97}Mo/^{95}Mo, ^{98}Mo/^{95}Mo and ^{100}Mo/^{95}Mo ratio measurements at the 95% confidence (2σ) level. The isotopic composition of Mo in another standard (Ultra Scientific standard, lot #D00811, N. Kingstown, RI 02852, USA) available in our laboratory was identical, within the limits of instrumental precision (Table 4).

Variations in Mo isotopic composition of synthetic mixtures with the in-house Mo standard, after purification by chromatographic column processing, are also within the precision limits stated above. This also provides further confirmation of the lack of artificially induced fractionation of Mo by the developed separation method.

3.5.2. Precision and accuracy of isotope ratio measurements for geological samples

A number of natural samples have been analyzed using the procedures described above. These include molybdenites from different localities and deposited sediments collected from two lakes in northern Sweden. The results are summarized in Table 4. δ^{97}Mo values for molybdenites from different localities in Sweden and China vary from −0.20 to 0.21‰ relative to our in-house Mo standard, consistent with the range reported for molybdenites in previous studies [17]. An important observation is that ^{97}Mo/^{95}Mo, ^{98}Mo/^{95}Mo and ^{100}Mo/^{95}Mo ratios for sediment samples that have been purified from concomitant matrix elements are very reproducible and mass dependent. But the results for ^{94}Mo/^{95}Mo (not shown here) and ^{96}Mo/^{95}Mo ratios were erratic for some sediment samples (samples from lake Vettasjärvi). We attribute this to interferences originating from residual matrix elements on ^{94}Mo and ^{96}Mo isotopes, notably ^{54}Fe^{40}Ar^{+} on ^{94}Mo^{+} and ^{56}Fe^{40}Ar^{+} on ^{96}Mo^{+} (see also Table 3). This conclusion is supported by the observation that, for the samples with ratio of Mo to Fe higher than 5, i.e., after very efficient purification, the measured isotopic data for ^{96}Mo/^{95}Mo are

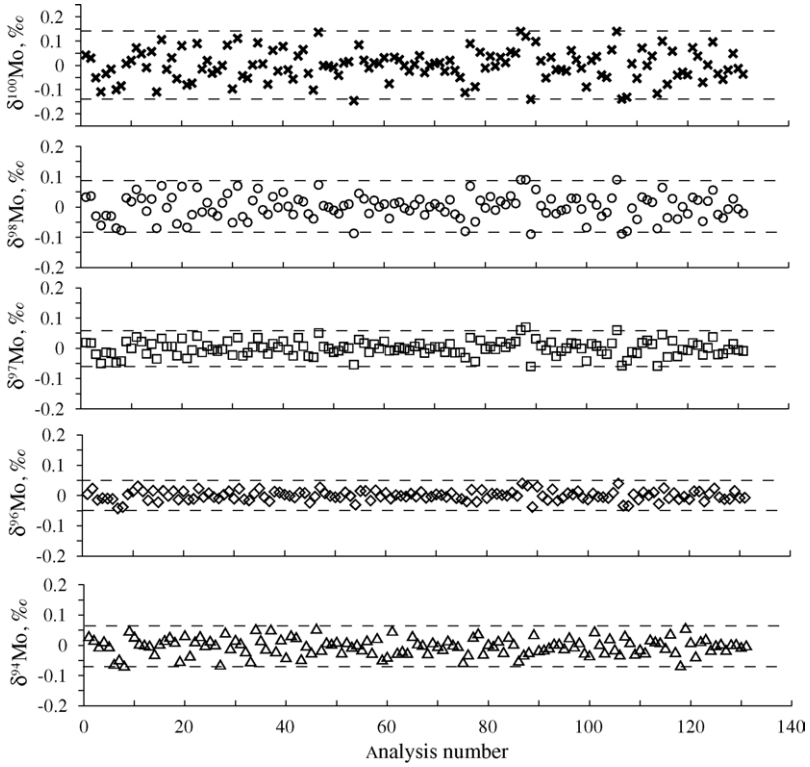

Fig. 5. Reproducibility of Mo isotope ratios for our in-house Mo standard during the course of nine measurement sessions. The measured solutions have Mo concentration of 1 mg l^{-1} and Pd of 0.5 mg l^{-1}. The isotope ratios were calculated in per mil relative to the same bracketing standards. The long-term reproducibility obtained defines an external precision of 0.06, 0.04, 0.06, 0.08 and 0.14‰ for ^{94}Mo/^{95}Mo, ^{96}Mo/^{95}Mo, ^{97}Mo/^{95}Mo, ^{98}Mo/^{95}Mo and ^{100}Mo/^{95}Mo ratio measurements at 95% confidence (2σ) level.

mass dependent relative to other Mo isotope ratios (Table 4, samples from lake Kutsasärvi). For some samples appreciable amounts of Zr were released to solution during the reductive HCl leach. This Zr was reduced to a near-blank level after purification, but not completely removed. In such cases, the isobaric interferences with Zr isotopes can contribute to disturbances of the measured ^{94}Mo^{+} and ^{96}Mo^{+} ion beams. The results therefore demonstrate that three Mo isotope ratios, ^{97}Mo/^{95}Mo, ^{98}Mo/^{95}Mo and ^{100}Mo/^{95}Mo, are most suitable for precise MC-ICPMS measurements of variations in isotopic composition of Mo in geological materials.

3.6. Isotopic variations of Mo in freshwater sediments: implication for global Mo isotope budget

As seen in Table 4, the variations of δ^{97}Mo values for freshwater sediment columns span an entire range of ~2.2‰. These variations show the existence of different Mo isotopic pools in freshwater lake systems. The geochemical implication of this finding is briefly discussed below, following characterization of sediments as revealed in this study.

The studied lakes are located in similar geomorphologic settings, neither having any significant sources of inflowing stream water. The difference in the depositional environments of the lakes is mainly due to the layer of anoxic bottom water developing in lake Vettasjärvi during winter time, when the ice cover acts as a barrier to diffusion of O_2 into the water. Concentrations of Mo in sediments of the lakes are enriched relative to the average upper crust abundance of 1–2 ppm [38]. This is apparently a reflection of the close proximity to copper porphyry-style mineral deposits (Aitik, northern Sweden) and abundant quartz–molybdenite veins and their dispersed remnants in the granitic till of the area. The proximity to a molybdenite source is known as the important factor controlling the distribution of Mo in lake sediments [39]. The dominant geochemical pathway for producing hydrous Fe and Mn oxides in these sediments is the precipitation of Fe and Mn from the water column or pore waters, where ferrous Fe and Mn(II) are oxidized. Both sediment columns have insignificant concentrations of sulfur. For the sediments of lake Vettasjärvi, sulfur concentrations range from 0.3 to 0.5%, whereas for those of lake Kutsasjärvi this range is from 0.05 to 0.2%.

Two dominant mechanisms of Mo removal in oxic and anoxic waters have been established in previous studies. These are the scavenging of Mo by Mn hydrous oxides in the former case and formation of particle reactive oxythiomolybdates ($MoO_{4-x}S_x^{2-}$) in the latter [2,4,5,40–42]. However, the mechanism of Mo removal in suboxic systems is unclear [40,41]. To explain Mo removal in suboxic settings, a two-layer diffusion-reaction model has been suggested, in which a reaction zone in the anoxic sediments, where Mo is

Table 4
Mo isotopic composition of molybdenites and deposited sediments analyzed in this study relative to our in-house Mo standard solution High Purity, Charlston, USA (lot #320304)

Sample	δ^{96}Mo	δ^{97}Mo	δ^{98}Mo	δ^{100}Mo
Ultra Scientific Mo standard solution, Kingston, USA, lot #D00811	−0.03 ± 0.02	−0.04 ± 0.03	−0.07 ± 0.04	−0.09 ± 0.07
HLP, China	−0.10 ± 0.02	−0.20 ± 0.03	−0.30 ± 0.03	−0.49 ± 0.03
JDC, China	0.06 ± 0.02	0.12 ± 0.03	0.16 ± 0.03	0.28 ± 0.03
Kåtaberget, Sweden	0.11 ± 0.02	0.21 ± 0.03	0.29 ± 0.03	0.47 ± 0.03
h (cm)	Lake Vettasjärvi			
1	n.d.	−0.62 ± 0.03	−0.91 ± 0.04	−1.44 ± 0.08
2	n.d.	−0.48 ± 0.03	−0.72 ± 0.03	−1.14 ± 0.05
3	n.d.	−0.46 ± 0.03	−0.69 ± 0.03	−1.12 ± 0.05
4	n.d.	−0.26 ± 0.03	−0.39 ± 0.03	−0.57 ± 0.05
5	n.d.	−0.63 ± 0.03	−0.91 ± 0.03	−1.45 ± 0.05
6	n.d.	−0.81 ± 0.03	−1.22 ± 0.03	−1.96 ± 0.05
7	n.d.	−0.61 ± 0.03	−0.90 ± 0.03	−1.48 ± 0.05
8	n.d.	−0.49 ± 0.03	−0.74 ± 0.03	−1.19 ± 0.09
9	n.d.	−0.70 ± 0.03	−1.04 ± 0.03	−1.69 ± 0.05
10	n.d.	−0.67 ± 0.03	−1.01 ± 0.03	−1.62 ± 0.05
11	n.d.	−0.82 ± 0.03	−1.21 ± 0.06	−1.94 ± 0.07
12	n.d.	−0.92 ± 0.03	−1.35 ± 0.04	−2.17 ± 0.06
	Lake Kutsasjärvi			
1	0.56 ± 0.03	1.01 ± 0.03	1.48 ± 0.04	2.43 ± 0.06
2	0.60 ± 0.03	1.10 ± 0.04	1.65 ± 0.05	2.70 ± 0.06
3	0.50 ± 0.03	0.96 ± 0.03	1.40 ± 0.03	2.31 ± 0.05
4	0.66 ± 0.03	1.26 ± 0.04	1.89 ± 0.04	3.10 ± 0.06
5	0.49 ± 0.03	0.92 ± 0.04	1.37 ± 0.07	2.26 ± 0.1
7	0.30 ± 0.03	0.56 ± 0.03	0.83 ± 0.03	1.35 ± 0.05
8	0.32 ± 0.03	0.62 ± 0.04	0.96 ± 0.04	1.61 ± 0.06
9	0.30 ± 0.03	0.55 ± 0.05	0.84 ± 0.04	1.36 ± 0.08
10	0.37 ± 0.03	0.71 ± 0.03	1.05 ± 0.03	1.71 ± 0.05
11	0.41 ± 0.03	0.83 ± 0.03	1.21 ± 0.04	1.98 ± 0.09
12	0.42 ± 0.03	0.81 ± 0.07	1.21 ± 0.08	1.95 ± 0.10
13	0.26 ± 0.03	0.40 ± 0.03	0.60 ± 0.03	0.98 ± 0.05
14	0.32 ± 0.03	0.52 ± 0.03	0.78 ± 0.04	1.30 ± 0.06
15	0.35 ± 0.03	0.64 ± 0.03	0.96 ± 0.04	1.56 ± 0.06
16	0.11 ± 0.03	0.17 ± 0.04	0.24 ± 0.04	0.46 ± 0.06
25	0.06 ± 0.03	0.08 ± 0.04	0.12 ± 0.04	0.26 ± 0.06

The depth of sediment layers is relative to the sediment surface. Uncertainty terms are one standard deviation.

chemically removed, is separated from the water column by a pure diffusive zone in which there is no chemical reaction [4,5]. An important consequence of such a model is that Mo isotope fractionation can be driven both by a specific isotope effect between MoO_4^{2-} and $MoO_{4-x}S_x^{2-}$ because of substantial differences in Mo bonding environments between such complexes and by relative fluxes of the isotopes across the sediments–water interface [2]. Rodushkin et al. [43] have demonstrated that diffusion of Fe and Zn in aqueous solution alone can cause changes in the studied $^{56}Fe/^{54}Fe$ and $^{66}Zn/^{64}Zn$ isotope ratios in excess of 0.3‰ in favour of the lighter isotope. The same "diffusional" mechanism might be expected for Mo isotopes as well.

The oxic–anoxic interface in lake Vettasjärvi is located in the water column. Hydrous Fe and Mn oxides produced by oxidation of dissolved Fe(II) and Mn(II) fluxes are precipitated to the sediment. Fig. 6 shows that concentrations of Mo, Fe_2O_3 and MnO_2 increase toward the bottom of the column, but do not exhibit large variations. δ^{97}Mo values vary from −0.25 to −0.95‰ and have a strong reverse correlation with Mo concentration. Molybdenum has a high affinity for particulate Mn oxides and is adsorbed essentially on their surfaces. It has also been demonstrated that Mo adsorbed on the surface of Mn oxides is enriched in the lighter isotopes [13,16]. These studies demonstrated that the isotopic data show a close system exchange between adsorbed and dissolved Mo. δ^{97}Mo values for adsorbed Mo relative to the Mo standard at semi-neutral pH ranged between −0.5 and −1.0‰ and a mean δ^{97}Mo offset of ∼1.8‰ was observed between dissolved and oxide-bound Mo [2,16]. Under anoxic conditions, Mn oxides are subject to reductive dissolution. Molybdenum released to pore waters upon reduction of Mn oxides is available for diffusive transport to the deeper layers of the sediment. The isotope effects for the dissolved Mo in

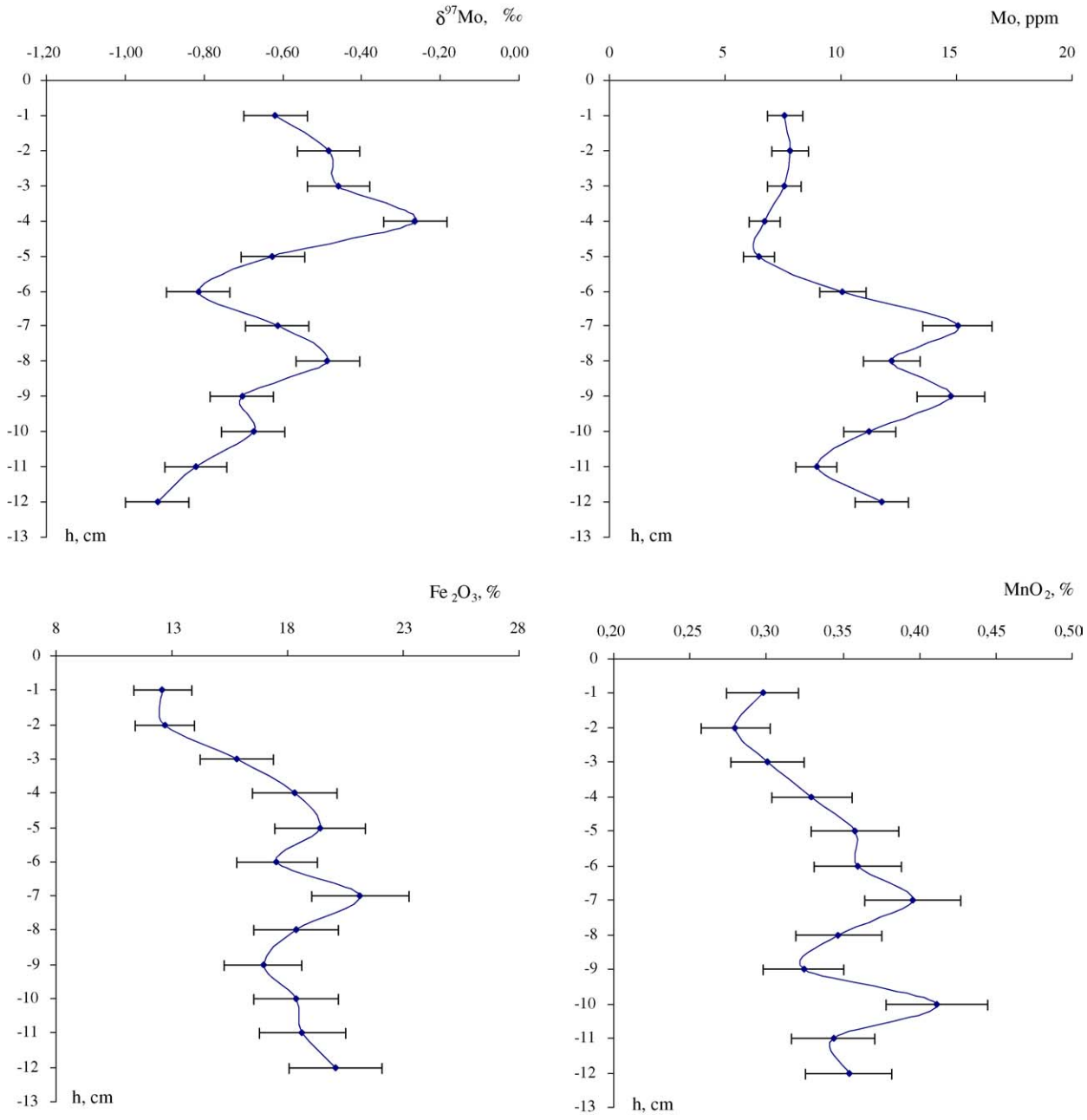

Fig. 6. Vertical profiles of δ^{97}Mo values, Mo, MnO_2 and Fe_2O_3 contents for sediment column of lake Vettasjärvi, northern Sweden. Uncertainty bars are two standard deviations.

pore waters can be produced by diffusion as suggested above, and interactions with solid surfaces and organic matter. The distribution of δ^{97}Mo values in the sediment column of lake Vettasjärvi is consistent with such explanation, though identifying the dominant control is difficult due to many unknowns.

Lake Kutsasjärvi is a permanently oxygenated lake. The oxic–anoxic interface in this case is situated in the sediment column. Concentrations of Fe_2O_3, MnO_2 and Mo in the column are subject to large variations (Fig. 7). The sharp concentration peak of Fe_2O_3 at a depth of 11 cm might be interpreted as a transition zone between anoxic and oxic environments, where dissolved ferrous species diffusing upwards along concentration gradients in the pore waters become oxidized and precipitated as hydrous Fe oxides. An interesting observation is that the concentration of Mo is strongly correlated with Fe_2O_3. The remarkable peak of Mo concentration accompanies that of Fe_2O_3. δ^{97}Mo values for this column have a tendency of decreasing toward the bottom from 1.26 to 0.08‰. Variations in δ^{97}Mo values are coupled with those for Fe_2O_3 and MnO_2.

The findings of the study indicate the necessity to quantify Mo isotope effects due to Mo interactions with organic matter and Fe oxides during geochemical cycling of Mo. Recently, a large body of evidence has appeared indicating

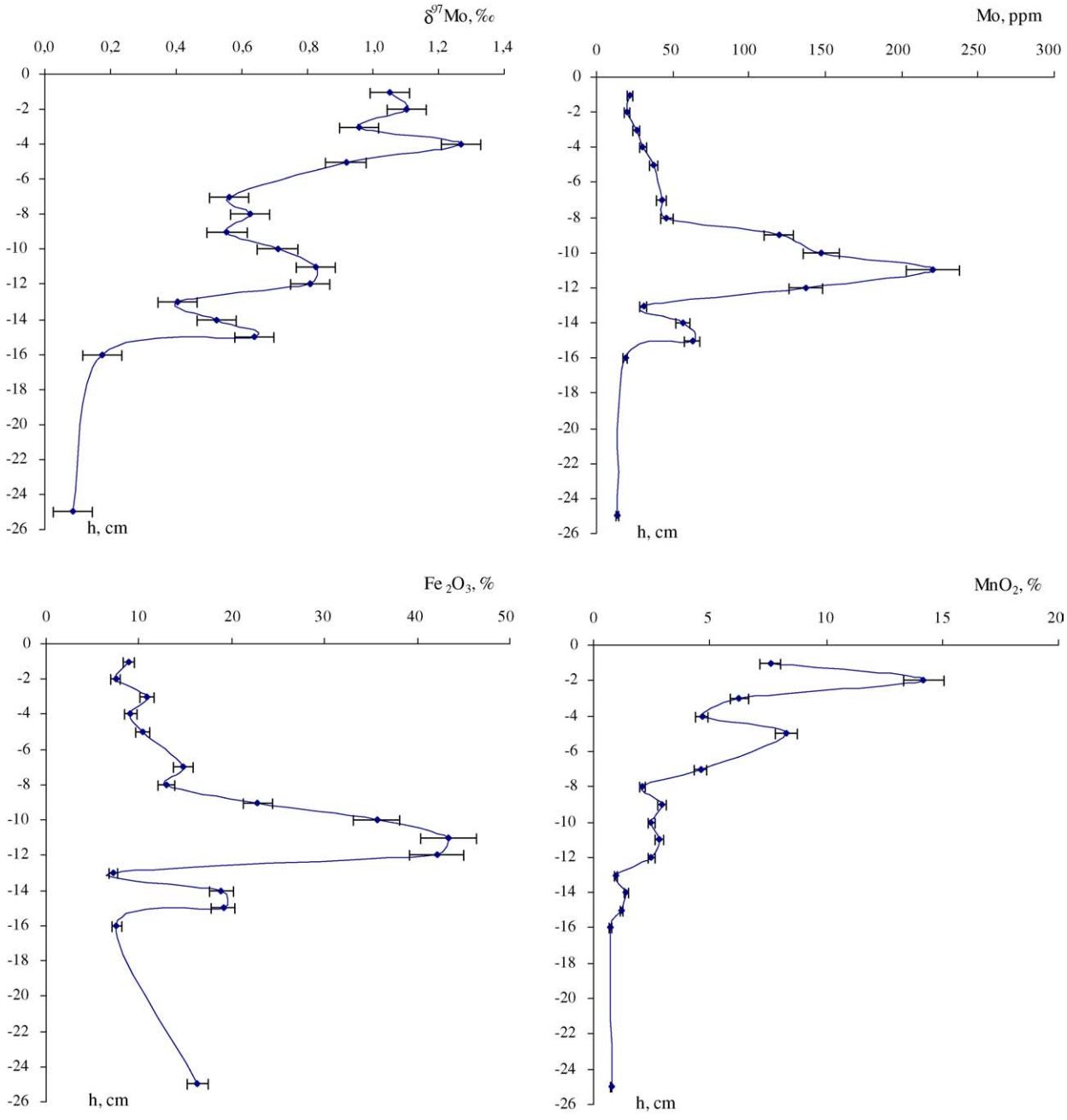

Fig. 7. Vertical profiles of δ^{97}Mo values, Mo, MnO_2 and Fe_2O_3 contents for sediment column of lake Kutsasjärvi, northern Sweden. Uncertainty bars are two standard deviations.

that, apart from Mn oxides, organic matter and Fe oxides exert a substantial role in Mo distribution in oxygenated waters [39,42,44]. From the data presented above it might also be speculated that geochemical processes operating during continental weathering and transport of Mo to the ocean produce a Mo isotope signature that is significantly different from that of the bedrock within the drainage basins. Furthermore, systematic variations in Mo isotopic composition of continental run-off might reflect certain geochemical conditions of the drainage basin. Variations of Mo isotopic composition due to these processes have to be studied in detail in order to be able to interpret the global Mo isotopic budget and make use of stable Mo isotopes as a proxy for redox conditions existed in geological past.

4. Conclusions

A new MC-ICPMS technique reported here make it possible to measure four Mo isotope ratios, ^{96}Mo/^{95}Mo, ^{97}Mo/^{95}Mo, ^{98}Mo/^{95}Mo and ^{100}Mo/^{95}Mo, to high precision and accuracy. Advantages of the technique over previous

MC-ICPMS methods include (i) a novel efficient purification chemistry of Mo that allows the efficient separation of Mo from Fe and other concomitant matrix elements and (ii) a MC-ICPMS measurement protocol that allows interference-free measurement of the aforementioned Mo isotope ratios utilizing correction for mass bias using external normalization to the $^{105}Pd/^{104}Pd$ ratio. It is anticipated that this new technique offers wide potential in geochemical and other fields of Mo isotope research.

The isotopic analysis of Mo for two freshwater sediment columns revealed that variations of $\delta^{97}Mo$ values span an entire range of ~2.2‰. These findings highlight the necessity to quantify isotope effects of Mo produced by geochemical processes operating during continental weathering and transport of Mo to the oceans. Variations in Mo isotopic composition of continental run-off might therefore be coupled with certain geochemical conditions of the drainage basin and can be used in reconstructions of geochemical environments existed in the past.

Acknowledgements

This research was supported by grants from EU's structural fund for Objective 1 Norra Norrland. The Neptune MC-ICPMS instrument was purchased through a grant from Kempestiftelsen. We would like to thank Johan Gelting-Niström and Jerry Forsberg for their assistance in sample collection, as well as Lars Gunneriusson for input on Mo speciation in acidic solutions. Thanks are due to the Centre for Isotope and Trace Element Measurement at Luleå University of Technology for support. Christer Pontér, Emma Engström and staff of Analytica AB are gratefully acknowledged for technical assistance.

References

[1] J.R. De Laeter, J.K. Böhlke, P. De Bièvre, H. Hidaka, H.S. Peiser, K.J.R. Rosman, P.D.P. Taylor, Pure Appl. Chem. 75 (2003) 683.
[2] A.D. Anbar, Rev. Miner. Geochem. 55 (2004) 429.
[3] K. Bertine, K. Turekian, Geochim. Cosmochim. Acta 37 (1973) 1415.
[4] S.R. Emerson, S.S. Huested, Mar. Chem. 34 (1991) 177.
[5] J. Crusius, S. Calvert, T. Pedersen, D. Sage, Earth Planet. Sci. Lett. 145 (1996) 65.
[6] W.E. Dean, J.V. Gardiner, D.Z. Piper, Geochim. Cosmochim. Acta 61 (1997) 4507.
[7] W.E. Dean, D.Z. Piper, L.C. Peterson, Geology 27 (1999) 507.
[8] K.W. Bruland, in: J.P. Riley, R. Chester (Eds.), Chemical Oceanography, vol. 8, Academic Press, London, 1983, p. 157.
[9] D.-C. Lee, A.N. Halliday, Int. J. Mass Spectrom. Ion Process. 146/147 (1995) 35.
[10] M. Wieser, J.R. De Laeter, Int. J. Mass Spectrom. 197 (2000) 253.
[11] A.D. Anbar, K.A. Knab, J. Barling, Anal. Chem. 73 (2001) 1425.
[12] C. Siebert, T.F. Nägler, J.D. Kramers, Geochem. Geophys. Geosyst. 2 (2001), 2000GG000124.
[13] J. Barling, G.L. Arnold, A.D. Anbar, Earth Planet. Sci. Lett. 193 (2001) 447.
[14] J. McManus, T.F. Nägler, C. Siebert, C.G. Wheat, D.E. Hammond, Geochem. Geophys. Geosyst. 3 (2002), 2002GG000356.
[15] C. Siebert, T.F. Nägler, F. von Blanckenburg, Earth Planet. Sci. Lett. 211 (2003) 159.
[16] J. Barling, A.D. Anbar, Earth Planet. Sci. Lett. 217 (2004) 315.
[17] M. Wieser, J.R. De Laeter, Int. J. Mass Spectrom. 225 (2003) 177.
[18] F. Albarède, B. Beard, Rev. Miner. Geochem. 55 (2004) 113.
[19] F. Albarède, P. Telouk, J. Blichert-Toft, M. Boyet, A. Agranier, B. Nelson, Geochim. Cosmochim. Acta 68 (2004) 2725.
[20] N. Dauphas, L. Reisberg, B. Marty, Anal. Chem. 73 (2001) 2613.
[21] A. Stenberg, D. Malinovsky, I. Rodushkin, H. Andren, C. Pontér, B. Öhlander, D.C. Baxter, J. Anal. At. Spectrom. 18 (2003) 23.
[22] S. Weyer, J.B. Schwieters, Int. J. Mass Spectrom. 226 (2003) 355.
[23] R. Markey, H. Stein, J. Morgan, Talanta 45 (1998) 935.
[24] D. Malinovsky, I. Rodushkin, D.C. Baxter, B. Öhlander, Anal. Chim. Acta 463 (2002) 111.
[25] K. Boström, L. Wiborg, J. Ingri. Mar. Chem. 50 (1982) 1.
[26] M. Kersten, U. Forstner, in: G. Batley (Ed.), Trace Element Speciation: Analytical Methods and Problems, CRC Press, 1989, p. 245.
[27] J.P. Riley, D. Taylor, Anal. Chim. Acta 41 (1968) 175.
[28] G. Schmuckler, Talanta 10 (1963) 745.
[29] H.M. Kingston, I.L. Barnes, T.J. Brady, T.C. Rains, Anal. Chem. 50 (1978) 2064.
[30] M. Pesavento, R. Biesuz, M. Gallorini, A. Profumo, Anal. Chem. 65 (1993) 2522.
[31] A. Yuchi, T. Sato, Y. Morimoto, H. Mizuno, H. Wada, Anal. Chem. 69 (1997) 2941.
[32] D. Atzei, T. Ferri, C. Sadun, P. Sangiorgio, R. Caminiti, J. Am. Chem. Soc. 123 (2001) 2552.
[33] G. Hägg, Allmän och Oorganisk Kemi, eighth ed., Almqvist & Wiksell, Uppsala, 1984, p. 665.
[34] J. Aveston, E.W. Anacker, J.S. Johnson, Inorg. Chem. 3 (1964) 735.
[35] C. Maréchal, P. Telouk, F. Albarède, Chem. Geol. 156 (1999) 251.
[36] E.D. Young, A. Galy, H. Nagahara, Geochim. Cosmochim. Acta 66. (2002) 1095.
[37] J.R. Hulston, H.G. Thode, J. Geophys. Res. 70 (1965) 3475.
[38] S.R. Taylor, S.M. McLennan, The Continental Crust: Its Composition and Evolution, Blackwell, Boston, 1985.
[39] S.J. Cook, J. Geochem. Explor. 71 (2000) 50.
[40] J. Morford, S. Emerson, Geochim. Cosmochim. Acta 63 (1999) 1735.
[41] T.J. Nameroff, L.S. Balistrieri, J.W. Murray, Geochim. Cosmochim. Acta 66 (2002) 1139.
[42] T.K. Dalai, K. Nishimura, Y. Nozaki, Chem. Geol. 218 (2005) 189.
[43] I. Rodushkin, A. Stenberg, H. Andrén, D. Malinovsky, D.C. Baxter, Anal. Chem. 76 (2004) 2148.
[44] M. Kracher, W. Shotyk, J. Environ. Monit. 6 (5) (2004) 418.